Evaluation of AHRS Algorithms for Inertial Personal Localization in Industrial Environments

Estefania Munoz Diaz and Fabian de Ponte Müller
German Aerospace Center (DLR)
Institute of Communications and Navigation
Oberpfaffenhofen, 82234 Wessling, Germany
Email: {Estefania.Munoz, Fabian.PonteMueller}@dlr.de

Antonio R. Jiménez and Francisco Zampella
Centre for Automation and Robotics (CAR)
Consejo Superior de Investigaciones Científicas (CSIC)-UPM
Ctra. Campo Real km 0.2, 28500 La Poveda,
Arganda del Rey, Madrid, Spain
Email: {antonio.jimenez, francisco.zampella}@csic.es

***Abstract*—This paper presents a comparison among several state-of-the-art Attitude and Heading Reference Systems (AHRS). These algorithms can be used for 3D orientation and position estimation of users or devices. The robust performance of these AHRS algorithms is of paramount importance, specially in environments with potential external perturbations, such as industrial environments. The comparison among AHRS algorithms presented in this paper also includes an algorithm recently proposed by the authors (DLR-AHRS). In this paper the performance of the different AHRS will be studied, including the effect of magnetic perturbations on the performance of orientation estimation, and the effect of using different patterns of motion when the sensor is carried by a user at different locations (pocket, foot/shoe, hand). These AHRS algorithms are also compared with the Kalman-based commercially available AHRS algorithm of Xsens. The performance of the AHRS algorithms depends strongly on the strategies used to reject perturbations (sudden accelerations or deformations of the Earth magnetic field) and the ability of the systems to estimate the biases of the gyroscopes.**

I. Introduction

The localization and navigation of personnel in industrial environments is a topic of interest that has a clear potential to improve the efficiency in the manufacturing processes, and to increase the safety of the staff when they interact with machines. The localization of users in an industrial environment is a challenging problem due to the lack of GNSS (GPS, GLONASS, Galileo, etc.) signals, since the building's structure blocks the satellite line-of-sight. Alternative methods to GNSS localization exist for indoor localization. They are based on a hybridization of local beacon-based positioning systems and Inertial Measurements Units (IMU) carried by the users. The position accuracy strongly depends on the quality of the sensor and the ability to estimate the sensor's orientation in a robust way. The industrial environment is specially challenging since magnetic perturbations, caused by motors and metallic parts, cause significant errors in the estimated orientation angles. This angular errors produce an increasing positioning error due to the integrative nature of dead-reckoning algorithms.

In the literature several authors combine in an appropriate way the measurements from an IMU (accelerometers and gyroscopes) and a magnetometer, as a way to obtain accurate estimates of the orientation. These sensors are known as a MARG (Magnetic, Angular Rate, and Gravity) units or MIMU (Magnetic and Inertial Measurement Unit). The combination of gyroscope and magnetic compass has been widely applied to obtain the heading [1], [2]. The integration of the gyroscope measurements, from a known initial orientation, provides the change in orientation. However, due to the gyroscope noise and biases, there is a long-term drift that needs to be corrected. The magnetometer, once calibrated, is used to limit or reduce the drift in the horizontal orientation. Additionally, the short-term accuracy of the gyroscope allows the detection of short-term external disturbances in the magnetic field that are usual in industrial environments.

Previous work in the area [3]–[5] treats the determination of the complete orientation, i.e. the estimation of the three Euler angles (roll, pitch and yaw), simultaneously. To obtain the orientation, an algorithm called Attitude and Heading Reference Systems (AHRS) combines the accelerometer, gyroscope and magnetometer measurements. Two absolute fields, the Earth magnetic field and the gravity field, whose directions and intensities are known, help estimating the orientation.

Several AHRS algorithms exist in the literature, some of them proprietary, but it has been observed that there is not a correct comparison among them, specially in the presence of magnetic perturbations. This paper presents a comparison among several known AHRS algorithms, studying the effect of magnetic perturbations on the performance of orientation estimation, and the effect of using different patterns of motion when a MIMU is carried at different locations (pocket, foot/shoe, hand).

II. Attitude and Heading Estimation Methods

An AHRS is an algorithm that provides the complete orientation of the sensor with respect to a navigation frame. The orientation is commonly represented with the Euler angles: roll, pitch and yaw.

A. AHRS Fundamental Approach

The objective of an AHRS algorithm is to optimally combine the information from gyroscopes, accelerometers and magnetometers to obtain the orientation. An AHRS algorithm is conceptually divided in two separated blocks: 1) orientation from gyroscopes, and 2) orientation from accelerometer and magnetometers. Both blocks give an

978-1-4799-7799-4/15/$31.00 ©2015 IEEE

independent orientation estimate, but accurate ARHS algorithms should integrate both approaches into a fused solution taking into account the benefits of each source of information. In the following section we will give the key concepts behind each block:

1) Orientation from Gyroscopes: Using a gyroscope and measuring the angular rate in sensor frame $\omega^s = (\omega_x^s, \omega_y^s, \omega_z^s)$, it is possible to estimate the orientation of the MIMU. This is achieved by accumulating the change of orientation derived from the gyroscope readings.

A rotation matrix or direction cosine matrix is a 3x3 matrix, in which each column is a rotation along the sensor axes specified in terms of the navigation axes. Rotation matrix, Euler angles and quaternions are analogue ways of representing the orientation.

Let $C(t)$ represent the rotation matrix at time t. Therefore the change of orientation is

$$\dot{C} = \lim_{\delta t \to 0} \frac{C(t+\delta t) - C(t)}{\delta t}. \tag{1}$$

For convenience, $C(t+\delta t)$ can be written as the product of two matrices in the following way

$$C(t+\delta t) = C(t) \cdot A(t), \tag{2}$$

being $A(t)$ the rotation matrix relating the time t and $t+\delta t$ in sensor frame.

If the sensor has experienced a small rotation, a small angle approximation can be applied yielding

$$A(t) = I + \delta\Psi. \tag{3}$$

Due to the high sampling frequency, the small angle approximation is valid. The matrix $\delta\Psi$ represents these small rotations. In the limit this matrix is equivalent to

$$\lim_{\delta t \to 0} \frac{\delta\Psi}{\delta t} = \Omega(t) \tag{4}$$

where $\Omega(t)$ represents the skew symmetric form of the angular rate vector ω^s.

Taking this into account, the change in orientation of Equation (1) yields

$$\dot{C} = C(t) \cdot \Omega(t) \tag{5}$$

and integrating both parts of the equation

$$C(t) = C(0) \cdot exp\left(\int_0^t \Omega(\tau) d\tau\right) \tag{6}$$

being $C(0)$ the initial orientation of the sensor.

2) Orientation from Accelerometers and Magnetometers: The accelerometers embedded in the MIMU measure gravity field in magnitude and direction in sensor frame $a^s = (a_x^s, a_y^s, a_z^s)$. Likewise, the orthogonal magnetometers measure the Earth magnetic field in magnitude and direction in sensor frame $m^s = (m_x^s, m_y^s, m_z^s)$. Depending on the distribution of these two fields among the three axes of the MIMU, its orientation relative to the navigation frame can be estimated.

As a first approximation, we assume that the sensor is either at a stand still or moves at a constant velocity and therefore the accelerometers measure only the gravity vector. Further on, we assume a non-disturbed magnetic field and therefore the magnetometers only measure the Earth magnetic field.

The knowledge of the gravity field yields an estimation of the attitude angles

$$\phi = \tan\left(\frac{a_y^s}{a_z^s}\right)^{-1} \tag{7}$$

and

$$\theta = \tan\left(\frac{-a_x^s}{\sqrt{(a_y^s)^2 + (a_z^s)^2}}\right)^{-1}, \tag{8}$$

where ϕ represents the roll angle, θ represents the pitch angle and a_i^s for $i = x, y, z$ represents the acceleration measurement for the i-axis measured in the sensor frame. The heading only using the gravity field remains unobservable.

Likewise, the knowledge of the Earth magnetic field yields an estimation of the heading

$$\psi = \tan\left(\frac{-m_x^h}{m_y^h}\right)^{-1} \pm D, \tag{9}$$

where ψ is the heading and m_i^h where $i = x, y$ is the magnetic field intensity for the i-axis projected in the horizontal plane of the navigation frame. The variable D represents the declination angle.

3) Integrating Both Basic AHRS Blocks: The most basic solution for integrating the two independent orientation estimation algorithms (gyroscope-based and the acceleration/magnetic field approach) is a simple weighted mean. This can be expressed by

$$q_{fused}(k) = \gamma \cdot q_g(k) + (1-\gamma) \cdot q_{a/m}(k), \tag{10}$$

where $q_g(k)$ is the orientation estimated by the integration of the gyroscopes, at time k, and $q_{a/m}(k)$ is the orientation computed using the acceleration and magnetometer readings (Equations 7, 8 and 9), both expressed in their quaternion form. The parameter γ is the weight that must be optimally computed for proper performance.

B. Optimizied AHRS Algorithms

Some recent AHRS algorithms in the literature that fuse gyroscope and accelerometer/magnetometer information are the Madwick [6] and Mahony [7] methods. We will briefly describe them, since they will be part of our comparison assessment.

1) Madgwick AHRS: This method is based on a gradient descent optimization, which makes it possible to obtain the relative 3D orientation of the MIMU towards the gravity field based on accelerometer readings, and the orientation along the Earth magnetic field using the magnetometers. A parameter is used to control the rate of convergence to the orientation estimate by optimally weighting the contribution of each sensor. The algorithm uses numerical integration of the orientation data with a quaternion representation.

2) Mahony AHRS: This method is based on an explicit complementary filter that requires accelerometer, gyroscope and magnetometer outputs. Its structure is suitable for implementation on embedded hardware. It estimates as well the biases of the gyroscope.

C. Robustifying the AHRS Algorithms

The basic AHRS algorithm presented in section II-A, the Madwick and Mahony only estimate correctly the orientation under ideal conditions, i.e. no significant accelerations and no magnetic disturbances. In order to properly use the accelerometer information, only the gravity has to be measured. Any acceleration of the sensor will corrupt the attitude estimation. It is recommendable to use a zero acceleration detector to locate the periods of zero or close to zero acceleration where roll and pitch estimations are valid [8].

A robust AHRS estimator should use the information of the Earth magnetic field only if the absence of magnetic disturbances is previously checked. Even if magnetometer measurements are always available, in indoor environments and other challenging outdoor scenarios such as the vicinity of ferromagnetic materials, the magnetic field is distorted. It is recommendable to use a magnetic distortions detector for not using the magnetic information in the presence of distortions [8].

The main problem of the algorithm explained in Subsection II-A1 are the biases of the gyroscopes. This orientation estimation is stable and accurate in short term, however, due to the continuous integration of sensor noise and biases, the long term estimation is prohibitively drifted. Therefore, it is recommendable as well to estimate in the AHRS, not only the Euler angles, but the biases of the gyroscopes. The proposed model for the biases of the gyroscopes is deeply explained in our previous work [9].

In [8], an alignment and realignment method has been proposed. For identifying the alignment and realignment periods, the static periods detector proposed is necessary. During these periods, the biases of the gyroscopes can easily be estimated.

Ideally, the biases of the gyroscopes should also be estimated during the walk and not only when the user is standing. To do that, we propose the magnetic angular rate update (MARU), explained in our previous work [10]. This estimation of the biases requires a constant magnetic field, that is a more relaxed requirement than the non-perturbed magnetic field. In order to find the periods where the Earth magnetic field is constant, we propose a modification of the magnetic disturbances detector proposed in [8].

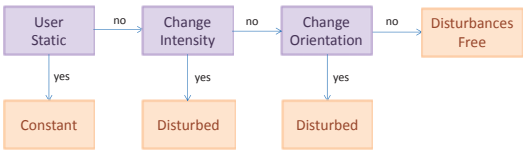

Fig. 1. Schema of the proposed improved magnetic disturbances detector.

Figure 1 shows the schema of the improved magnetic disturbances detector. Therefore, by using such a detector, the biases of the gyroscope can be as well estimated both, when the magnetic field is constant and when the magnetic field is disturbances free. During the period of disturbances free the yaw can also be estimated, as explained in Equation (9).

III. Comparison of AHRS Algorithms with Synthetic Signals

In order to evaluate the performance of the above described AHRS algorithms, i.e. Basic-AHRS, Madgwick, Mahony and DLR-AHRS, we created and used along this section a set of synthetic signals. These signals will allow us to make an initial assessment of the algorithms under test.

An evaluation using synthetic signals has several advantages, such as:

1) Providing a ground-truth for the roll, pitch and yaw angles, making it possible to compute the attitude estimation errors for different AHRS algorithm under a given synthetic test.
2) The ability to generate a diverse set of controlled perturbations, such as a set of displacements and turns with a wide bandwidth or the addition of some perturbing magnetic fields simulating indoor or industrial environments.
3) The possibility of using the ideal MIMU signals with the addition of controlled noise and biases.

A. Synthetic Signals

Since we want to verify the performance of the AHRS algorithms under diverse conditions, we have generated a single synthetic recording under different conditions, so we can distinguish several zones in the signal:

- *Zone A - Still*: In zone A the MIMU is totally still and leveled (so Euler angles are equal to zero)
- *Zone B - Rotations*: Includes alternative MIMU rotations in roll, pitch and yaw up to a maximum of 80 degrees (avoiding gimbal lock problem).
- *Zone C - Accelerations*: In zone C the MIMU is moved along the x, y and z-axis without any rotation with linear accelerations higher than gravity.
- *Zone D - Magnetic dipoles*: Several magnetic dipoles at different locations and with a given field intensity and direction, which are also moving with an oscillatory motion are included in zone D.
- *Zone E - Foot mounted*: This regions emulates the turn rates and acceleration perceived in a foot-mounted MIMU while walking.

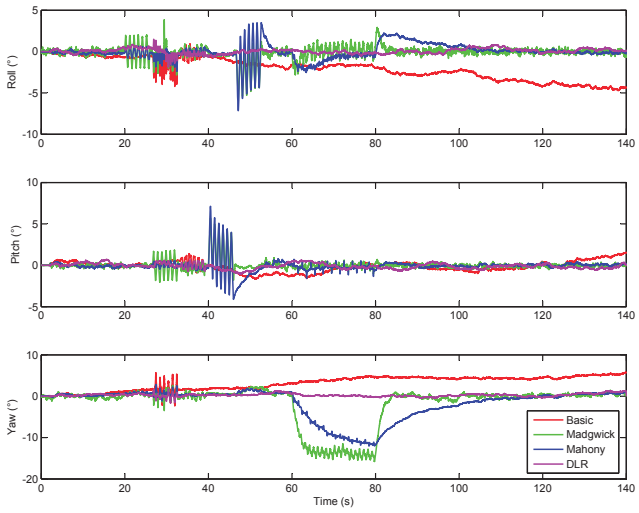

Fig. 3. Error in the different Euler angles for each AHRS algorithm under study with noisy signals.

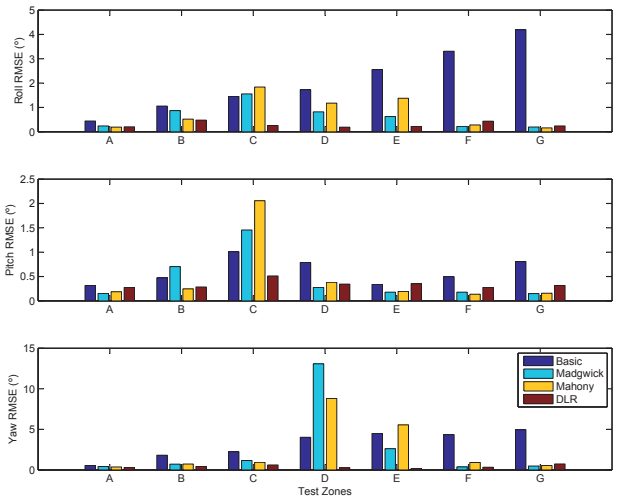

Fig. 4. RMSE of the error in the estimated Euler angles using different AHRS algorithms with noisy signals.

- *Zone F - Hand held*: This regions emulates the turn rates and acceleration perceived in a hand-held MIMU while walking.
- *Zone G - Pocket use*: This regions emulates the turn rates and acceleration perceived MIMU in the pocket while walking.

A short version of the simulated MIMU signals can be seen for illustration in Figure 2. In this case the zone A is in the time range (0-20 s), zone B is in (20-40 s), zone C is in (40-60 s), zone D is in (60-80 s), zone E is in (80-100 s), zone F is in (100-120 s), and zone G is in (120-140 s). The whole 3-axes acceleration signals are contaminated with additive zero-mean Gaussian noise (0.2 m/s^2). The gyroscope 3-axes signal has an additional 3 degrees per second noise and additional constant bias terms in x-y-z axes (-0.05, 0.05 and 0.1 ^{o}/s, respectively). The magnetometer has an added 0.1 Gauss standard deviation zero-mean gaussian noise.

B. Orientation Errors with Synthetic Signals

The evaluation of the different AHRS algorithms was done with a signal composed of 100 seconds per each individual zone (700 seconds in total). The results in form of errors for each particular Euler angle are shown in Figure 3

The root mean square error (RMS) of the angular error for each zone is shown in Figure 4 for the additive errors mentioned above. The RMSE errors are also included in Table I which also contains additional columns with rmse for other magnitudes of the zero-mean gaussian noise and the gyro biases (N1: noiseless signals; and N2: noisy signals with the above mentioned noise parameters). Last rows in this table show the mean RMSE for all zones ($\overline{RMSE}_z$), the RMSE for all zones and noises ($\overline{RMSE}_{zn}$), and the mean over all zones, noises and angles ($\overline{RMSE}_{zna}$).

It can be seen from Figure 4 and Table I that in general the pitch and roll angles are more accurate than the yaw angle, as expected. According to the magnetically degraded

Zone	Angle	AHRS Algorithm							
		Basic		Madgwick		Mahony		DLR	
		N1	N2	N1	N2	N1	N2	N1	N2
A	Roll	0.00	0.44	0.00	0.24	0.00	0.19	0.00	0.20
	Pitch	0.00	0.32	0.00	0.15	0.00	0.19	0.00	0.28
	Yaw	0.00	0.55	0.00	0.42	0.00	0.36	0.00	0.32
B	Roll	0.01	1.06	0.81	0.87	0.24	0.52	0.04	0.48
	Pitch	0.01	0.47	0.79	0.70	0.17	0.25	0.05	0.29
	Yaw	0.01	1.82	0.72	0.71	0.08	0.73	0.00	0.44
C	Roll	0.02	1.45	1.46	1.56	1.81	1.84	0.02	0.26
	Pitch	0.02	1.01	1.43	1.46	2.00	2.06	0.02	0.51
	Yaw	0.03	2.24	0.72	1.17	0.52	0.94	0.00	0.61
D	Roll	0.00	1.73	0.94	0.82	0.98	1.18	0.00	0.19
	Pitch	0.00	0.79	0.28	0.28	0.44	0.38	0.00	0.34
	Yaw	0.05	4.03	12.39	13.08	9.47	8.81	0.00	0.25
E	Roll	0.00	2.56	0.45	0.63	1.53	1.38	0.00	0.22
	Pitch	0.00	0.34	0.05	0.18	0.12	0.20	0.00	0.35
	Yaw	0.00	4.51	1.79	2.62	5.80	5.55	0.00	0.19
F	Roll	0.00	3.31	0.06	0.22	0.29	0.28	0.00	0.44
	Pitch	0.00	0.50	0.00	0.18	0.01	0.14	0.00	0.28
	Yaw	0.00	4.34	0.02	0.37	0.91	0.92	0.00	0.33
G	Roll	0.00	4.19	0.06	0.20	0.05	0.16	0.00	0.24
	Pitch	0.00	0.81	0.00	0.15	0.00	0.16	0.00	0.32
	Yaw	0.00	4.95	0.02	0.48	0.15	0.55	0.00	0.74
$\overline{RMSE}_z$	Roll	0.01	2.11	0.54	0.65	0.52	0.79	0.01	0.29
	Pitch	0.01	0.60	0.36	0.44	0.37	0.48	0.01	0.34
	Yaw	0.01	3.21	2.24	2.69	1.72	2.55	0.00	0.41
$\overline{RMSE}_{zn}$	Roll	0.31		0.59		0.66		0.15	
	Pitch	0.31		0.40		0.43		0.17	
	Yaw	1.61		2.46		2.14		0.21	
$\overline{RMSE}_{zna}$	All	0.99		1.15		1.07		0.18	

TABLE I
RMSE FOR THE DIFFERENT AHRS ALGORITHMS AND TESTING ZONES.

zone (D) the performance of the AHRS is better for the Basic-AHRS and DLR-AHRS algorithm since they contain a magnitude-based acceleration and magnetometer perturbation detector. However the Basic-AHRS algorithm is not capable of optimally integrating the gyroscope readings which are perturbed with biases, and therefore accumulates drift. In general terms, considering the average of the different zones in the noisy signals, the performance of the optimal algorithms is similar among them, being considerably better for the DLR-

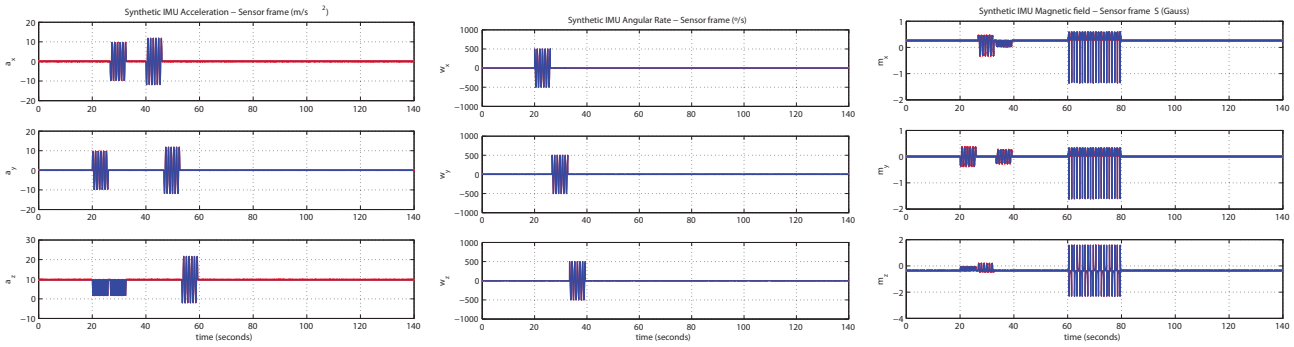

a) Acceleration b) Angular rate c) Magnetic field

Fig. 2. This figure represents the generated synthetic MIMU signals for accelerometers, gyroscopes and magnetometers. Each different zone lasts 20 seconds.

AHRS algorithm.

Next section will explore the performance of these AHRS algorithms using real signals, an with an additional AHRS algorithm (the one embedded in the XSens commercial sensor).

IV. Comparison of AHRS Algorithms with Xsens MIMU Signals

After the previous analysis with synthetic signals, we have carried out a set of measurements using the medium-cost MIMU MTw from Xsens. The advantage of using these signals is that we can assess the previous analysis with real sensors and we can also compare the available orientation solution provided by Xsens with the AHRS algorithms previously explained.

We have divided this analysis in two parts: a non-perturbed environment and a magnetically perturbed environment. The non-perturbed environment tests were carried out in the middle of a football field, free of metallic objects or electric current cables. Before doing these tests, the MIMU was calibrated at the same place. As indicated in [8], the calibration of the magnetometers is of high importance.

The non-perturbed environment tests consist of a 24 meters long square shaped walk. In order to evaluate the drift in the heading angle, the starting and ending point are chosen to have the same heading. These tests have been performed with the MIMU in the pocket and held in the hand. The next figures show the performance comparison of the commercially available Xsens heading solution, the previously described DLR and Basic AHRS algorithms and Madgwick and Mahony AHRS methods.

Figure 5 shows the yaw angle for both, Xsens and DLR AHRS algorithms. Both methods show a similar performance regarding the accumulation of heading error and the results are similar for different realizations. Figure 6 shows that, as expected from the synthetic analysis, the performance of these AHRS algorithms is comparable to the Xsens and DLR. For the hand held location, the Madgwick and Mahony methods found the initial yaw to be around $-120°$, although they were initialized at $0°$. This is because they use the absolute magnetic field for computing the orientation, as previously explained.

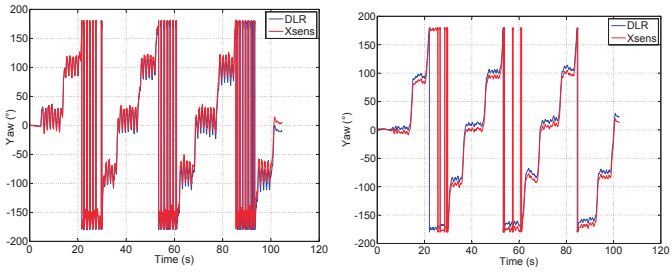

(a) Pocket location (b) Hand held location

Fig. 5. Comparison of heading estimation in a non-perturbed environment for DLR and Xsens AHRS algorithms.

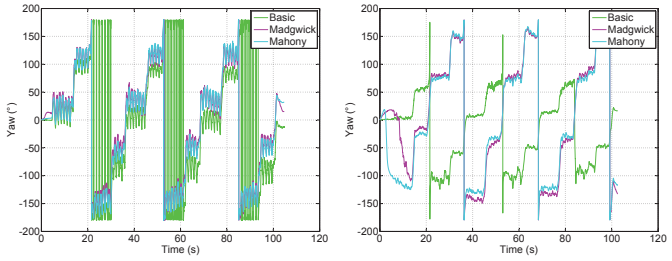

(a) Pocket location (b) Hand held location

Fig. 6. Comparison of heading estimation in a non-perturbed environment for Basic, Madgwick and Mahony AHRS methods.

The rest of the algorithms assume that the initial yaw is equal to $0°$ and keep the estimation relative to the initial value.

For the perturbed environment we have used a ground-truth signal as reference. We have used the fiber optic gyroscope (FOG) DSP-1750 from KVH. As explained in [8], the Allan variance analysis of the FOG reveals that it can be used as a reference for the orientation. For measuring with both sensors, FOG and Xsens MIMU, we attach the Xsens with tape to the flat part of the FOG. For the pocket experiments FOG and the Xsens were attached to the thigh of the user.

Before recording magnetic data with the Xsens MIMU, it is necessary to calibrate it once more, since the metallic materials of the attached FOG and screws produce soft iron effects that bias the magnetometer measurements. The calibration parameters of the MIMU magnetometers with and without the

FOG attached are shown in Table II and their difference give evidence of the perturbations that the metallic parts cause. The magnetometer measurements $m_i^s(meas)$ yield the calibrated measurements $m_i^s(cal)$ with

$$m_i^s(cal) = B_{real}(\frac{1}{B_{field}} \cdot m_i^s(meas) + O_i), \qquad (11)$$

where B_{real} is 0.482 Gauss in the case of Munich, B_{field} is a scaling factor and O_i is the offset of each axis.

	B field	offset X	offset Y	offset Z
MIMU	0.9475	-0.0946	-0.0877	-0.1586
MIMU+FOG	0.9396	-0.1079	-0.1155	-0.1191

TABLE II
DIFFERENT VALUES FOR THE MIMU MAGNETOMETERS CALIBRATION.

Due to its great accuracy, to use the FOG as a reference for evaluating the performance of the different AHRS methods, it is sufficient to integrate its gyroscope signals according to Equation (6). Longer experiments require to apply corrections for the Earth rotation. Due to the limited area in which the experiments take place a transport rate correction is not needed.

In the following figure we show the error for the heading by subtracting the different AHRS algorithms' solution from the FOG reference solution and the norm of the magnetic field measured during the walk.

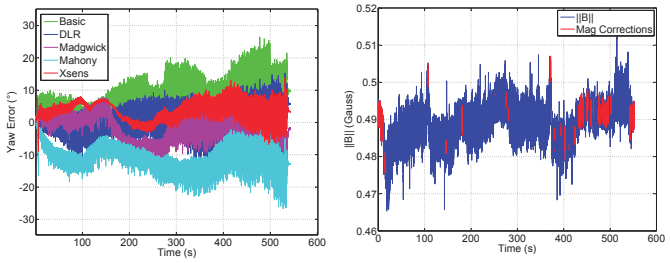

(a) Error in the yaw angle estimation. (b) Norm of the magnetic field.

Fig. 7. This figure represents the error in the yaw angle and the norm of the magnetic field. During the periods represented in red, the magnetic correction is applied.

Figure 7(a) shows the different heading errors of the AHRS algorithms. The errors in both, the Madgwick and Mahony AHRS methods, are probably caused by the magnetic field perturbations. Figure 7(b) shows in blue the norm of the magnetic field measured during the walk. The periods marked in red are disturbances-free or constant field periods detected by the magnetic disturbances detector. During these periods the magnetic updates are applied. The DLR-AHRS algorithm keeps an error around $0°$ with a standard deviation of $4°$ during the whole walk. As expected, this error increases with time.

V. CONCLUSIONS

This paper presents a comparison among several state-of-the-art AHRS algorithms, including the available commercial orientation solution of Xsens, two well-known open source methods namely Madgwick and Mahony, a basic AHRS estimation algorithm and the recently algorithm proposed by the authors. In this work the performance of the different AHRS algorithms has been studied, emphasizing the effect of magnetic perturbations. Different patterns of motion derived from carrying the MIMU at different locations such as pocket, foot/shoe and hand, have been studied. The results extracted of our analyses with synthetic signals, where all parameters are easily controllable, are confirmed by real measurements taken with the MTw MIMU of Xsens. We conclude that an algorithm to detect the magnetic perturbations is highly recommendable, however, for a non-perturbed magnetic field the performance of all AHRS algorithms studied is similar.

VI. ACKNOWLEDGEMENTS

The authors thank the financial support received from projects: LEMUR (TIN2009-14114-C04-03), LAZARO (CSIC-PIE Ref.201150E039) and LORIS (TIN2012-38080-C04-04).

REFERENCES

[1] J. W. Kim, H. J. Jang, D.-H. Hwang, and C. Park, "A step, stride and heading determination for the pedestrian navigation system," *Journal of Global Positioning Systems*, vol. 3, no. 1-2, pp. 273–279, 2004.

[2] P. Goyal, V. J. Ribeiro, H. Saran, and A. Kumar, "Strap-down pedestrian dead-reckoning system," in *Indoor Positioning and Indoor Navigation (IPIN), 2011 International Conference on*. IEEE, 2011, pp. 1–7.

[3] A. Kim and M. Golnaraghi, "A quaternion-based orientation estimation algorithm using an inertial measurement unit," in *Position Location and Navigation Symposium, 2004. PLANS 2004*. IEEE, 2004, pp. 268–272.

[4] E. Kraft, "A quaternion-based unscented kalman filter for orientation tracking," in *Proceedings of the Sixth International Conference of Information Fusion*, vol. 1, 2003, pp. 47–54.

[5] M. Wang, Y. Yang, R. R. Hatch, and Y. Zhang, "Adaptive filter for a miniature mems based attitude and heading reference system," in *Position Location and Navigation Symposium, 2004. PLANS 2004*. IEEE, 2004, pp. 193–200.

[6] S. Madgwick, "An Efficient Orientation Filter for Inertial and Inertial/Magnetic Sensor Arrays," *Report x-io and University of Bristol*, April 2010.

[7] R. Mahony, T. Hamel, and J.-M. Pflimlin, "Nonlinear Complementary Filters on the Special Orthogonal Group," *IEEE Transactions on Automatic Control, Institute of Electrical and Electronics Engineers (IEEE)*, pp. 1203–1217, May 2008.

[8] E. Munoz Diaz, A. L. Mendiguchia Gonzalez, and F. de Ponte Müller, "Standalone Inertial Pocket Navigation System," *IEEE/ION Position Location and Navigation Symposium, Monterey, USA*, pp. 241–251, May 2014.

[9] E. Munoz Diaz, O. Heirich, M. Khider, and P. Robertson, "Optimal Sampling Frequency and Bias Error Modeling for Foot-Mounted IMUs," *International conference on Indoor Positioning and Indoor Navigation (IPIN)*, October 2013.

[10] F. Zampella, M. Khider, P. Robertson, and A. Jiménez, "Unscented kalman filter and magnetic angular rate update (maru) for an improved pedestrian dead-reckoning," in *Position Location and Navigation Symposium (PLANS), 2012 IEEE/ION*. IEEE, 2012, pp. 129–139.